Available online at www.sciencedirect.com
ScienceDirect
International Journal of Thermal Sciences 47 (2008) 858–874
International Journal of Thermal Sciences
www.elsevier.com/locate/ijts

# Experimental and analytical investigation of solidification and melting characteristics of PCMs inside cylindrical encapsulation

S. Kalaiselvam [a,*], M. Veerappan [a], A. Arul Aaron [b], S. Iniyan [a]

[a] *Refrigeration and Air Conditioning Division, Department of Mechanical Engineering, Anna University, Chennai, India*
[b] *Swinburne University of Technology, Melbourne, Australia*

Received 29 March 2007; received in revised form 11 June 2007; accepted 4 July 2007

Available online 28 January 2008

**Abstract**

Phase change materials encapsulated inside cylindrical enclosures are analyzed for solidification and melting process. Analytical solutions for finding the interface locations at various time steps are obtained. Transient interface positions and complete phase change time is predicted by two models for solidification and by three models for melting. To validate the analytical results, experiments are carried out to find the transient positions of the front. The agreement was found to be good for model with conduction and heat generation in solidification process, but in melting the model with conduction, convection and heat generation gives a better prediction. Validated analytical model is extended to study the phase change behavior and heat transfer characteristics inside PCM. Presence of heat generation increases the total solidification time of the cylinder, though it accelerates melting. Total solidification time depends on Stefan number and heat generation parameter $\beta$, whereas complete melting time depends on equivalent thermal conductivity. This paper also analyzes the behavior of three paraffins, 60% *n*-tetradecane + 40% *n*-hexadecane, *n*-tetradecane, and *n*-pentadecane. Since the model considered the influence of heat generation, analytical predictions are also helpful in applications such as nuclear fuel freezing, microwave thawing, and vacuum freeze drying.


*Keywords:* Phase change; Energy storage; Solidification; Melting; Natural convection; Energy generation; *n*-alkanes

## 1. Introduction

Phase change materials (PCMs) have a strong ability to store energy and have an excellent characteristic of constant temperature in the course of absorbing or releasing energy. For the inward solidification processes, a number of researches have been revealed for the heat transfer as well as phase change phenomena. Solidification is normally considered as a pure conduction problem. On the other hand, melting process involves the natural convection effect of the liquid phase. But a literature inferred that there is a significant reduction in melting time for slab of ice due to the presence of heat generation [1], hence it is important to consider the presence of heat generation inside PCM. The influence of volumetric heat generation in PCM is of great importance in applications like laser melting of materials [2], vacuum freeze drying [3], microwave heating/thawing [4,5], nuclear fuel freezing [6,7] phase change solar collectors, biological tissues freezing. In spite of the impressive number of articles published on the subject over the last 15 years, only few publications deal with the effect of volumetric heat generation. Due to the nonlinearities of solid–liquid front, and limiting factors such as geometry, temperature variations, motions in the liquid phase, most of the research uses numerical or finite difference techniques. A numerical model to simulate a storage system and operational geometrical parameters of that system was investigated [8]. Finite difference method is applied to resolve the enthalpy equation [9–11]. Generally, transient heat equation was found to be best suited for addressing phase change phenomena. Solutions to the solid–liquid phase change phenomena are commonly referred as Stefan problem [1,3,12,13]. The application of moving boundary to single droplet drying was recently addressed and the temperature distribution was found to be significant inside the

* Corresponding author. Tel.: +91 44 2220 3262.
*E-mail addresses:* kalai@annauniv.edu (S. Kalaiselvam), veera_200@yahoo.co.in (M. Veerappan), aaron@alumni.swinburne.edu (A. Arul Aaron), iniyan_777@yahoo.com (S. Iniyan).

1290-0729/$ – see front matter 
doi:10.1016/j.ijthermalsci.2007.07.003

**Nomenclature**

| | | | |
|---|---|---|---|
| $c$ | Specific heat | J/kg K | |
| $Fo$ | Fourier number | | |
| $H$ | Latent heat of fusion | kJ/kg | |
| $k$ | Thermal conductivity | W/mK | |
| $k_{eq}(t)$ | Ratio of transferred heat rate by natural convection to that by thermal conduction | | |
| $Nu$ | Nusselt number | | |
| $q'''$ | Volumetric heat generation | $W/m^3$ | |
| $R$ | Radius of cylindrical capsule | m | |
| $s$ | Dimensionless position of the solid–liquid interface, defined in Eq. (6) | | |
| $Ste$ | Stefan number | | |
| $T$ | Temperature | °C | |
| $t$ | Time | s | |
| $x$ | Dimensionless co-ordinate | | |

*Greek symbols*

| | | |
|---|---|---|
| $\alpha$ | Thermal diffusivity | $m^2/s$ |
| $\beta$ | Dimensionless heat generation parameter | |
| $\theta$ | Dimensionless temperature | |
| $\lambda_{leq}(t)$ | Equivalent thermal conductivity of the liquid PCM | |
| $\xi$ | Spatial variable | m |
| $\rho$ | Density | $kg/m^3$ |
| $\sigma$ | Position of the interface in spatial variable | m |

*Subscripts*

| | |
|---|---|
| 0 | External fluid |
| cond | Conduction |
| conv | Convection |
| $f$ | Fusion |
| $L$ | Liquid phase |
| mel | Complete melting |
| $S$ | Solid phase |
| sol | Complete solidification |

droplet [14]. A simplified analytical model which predicts the solid–liquid interface location and temperature distribution of the fin in the solidification process is developed [15]. The effect of energy generation on freezing and melting in a semi-infinite region [16] and in slab geometry [1] was recently examined. There are numerous approximate analytical solutions based on various mathematical techniques such as variational approach, Megerlin method, perturbation, heat balance integral method and quasi-steady approximation for phase change problems with out considering heat generation. Almost all analytical solutions are limited to phase change materials initially at its melting temperature. But in actual, phase change materials will be at initial temperature greater than melting point or fusion temperature. Hence there is a need for analytic solutions to examine the effect of important parameters on solidification and melting of PCM in general, and on the solid–liquid interface motion in particular.

This paper considers the temperature of PCM initially above its fusion temperature. Phase change problems can be simplified by neglecting transient terms in the governing heat equation. The quasi-steady model developed in this paper is used to examine the effect of volumetric energy generation on one-dimensional solidification and melting of cylinder. Presence of energy generation reduces total melting time but it significantly increases total solidification time. The influence of Stefan number on the complete solidification time is also examined. Analytical solutions for finding the position of the moving interface at various time steps is given for both solidification and melting of cylinders with and without considering heat generation. Natural convection effect is also taken into account for melting problem. The solutions shows that complete solidification time depend on Stefan number and energy generation parameter. Developed analytical solutions are also validated experimentally, and it shows a good agreement between the experimental results and that predicted analytically. These analytical solutions can also be used to find complete solidification and melting time which helps in selection of phase change material with good charging and discharging characteristics.

## 2. Solidification analysis

Phase change materials can be encapsulated inside various cylindrical containments made up of glass, stainless steel, polyethylene, aluminum, or copper. To predict the characteristics behavior of moving boundary in the cylindrical capsules, single capsule of finite radius $R$ is considered for the analysis. Initially, cylinder is at a temperature $T_i$ above fusion temperature $T_f$, the surfaces of the cylinder $\xi = \pm R$ are maintained at a temperature $T_0 < T_f$. This problem can be resolved in two methods. Model I consists conduction and heat generation whereas model II assumes only conduction heat transfer. According to model I, the energy is generated throughout the cylinder at a constant volumetric rate $q'''$. Due to symmetry, the center line at $x = 0$ is insulated, and hence half of the cylinder is considered for analysis as shown in Fig. 1. Solidification starts on the surface of the cylinder, and moving solidification front forms instantaneously and propagates through the liquid phase. To simplify the problem, the changes of volume on solidification are neglected and the properties are same in both solid and liquid phases.

### 2.1. Model I (conduction and heat generation)

Based on these assumptions, the governing heat equations for solidification are,

$$\alpha\left(\frac{\partial^2 T_S}{\partial \xi^2} + \frac{1}{\xi}\frac{\partial T_S}{\partial \xi}\right) + \frac{q'''}{\rho c} = \frac{\partial T_S}{\partial t}, \quad \sigma \leqslant \xi \leqslant R \tag{1}$$

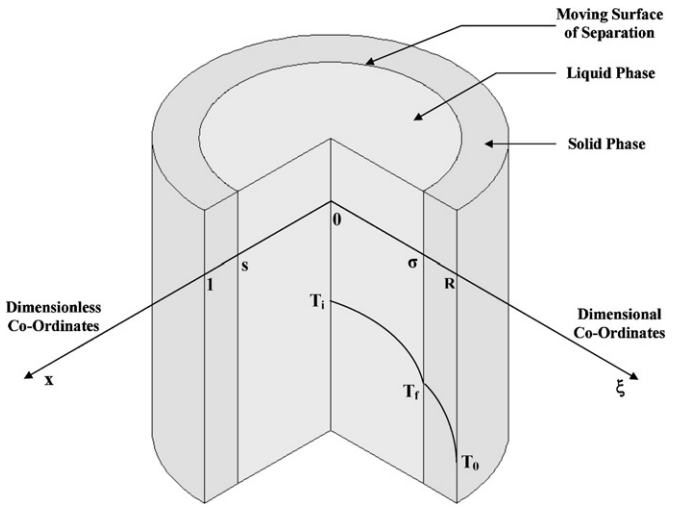


Fig. 1. Sectional model of the cylindrical PCM.

and

$$\alpha\left(\frac{\partial^2 T_L}{\partial \xi^2}+\frac{1}{\xi}\frac{\partial T_L}{\partial \xi}\right)+\frac{q'''}{\rho c}=\frac{\partial T_L}{\partial t},\quad 0\leqslant \xi\leqslant\sigma \tag{2}$$

where $\alpha$ is thermal diffusivity, $\rho$ is density, $c$ is specific heat, and the subscripts $S$ and $L$ represents solid and liquid phase, respectively. The boundary conditions are,

(1) $T_S(\xi=R,t)=T_0$.
(2) $T_S(\xi=\sigma,t)=T_f$.
(3) $T_L(\xi=\sigma,t)=T_f$.
(4) $\frac{\partial T_L(\xi=0,t)}{\partial x}=0$.

The initial conditions are,

(1) $T_L(\xi,t=0)=T_i$.
(2) $\sigma(t=0)=R$.

The interface energy balance between the solid and liquid phase along the solidification front,

$$k\frac{\partial T_S(\xi=\sigma,t)}{\partial \xi}-k\frac{\partial T_L(\xi=\sigma,t)}{\partial \xi}=\rho H\frac{\mathrm{d}\sigma}{\mathrm{d}t} \tag{3}$$

where $k$ is thermal conductivity, $H$ is latent heat of fusion, and $\sigma$ is solidification front position.

The dimensionless variables are adopted and the governing equation, boundary conditions, initial conditions and interface energy balance equation are cast in dimensionless form. The dimensionless quantities are,

$$x=\frac{\xi}{R},\quad \theta_S=\frac{T_f-T_S}{T_f-T_0},\quad \theta_L=\frac{T_f-T_L}{T_f-T_0},\quad s=\frac{\sigma}{R}$$

$$Fo=\frac{\alpha t}{R^2},\quad \beta=\frac{R^2 q'''}{k(T_f-T_0)} \tag{4}$$

Substituting non-dimensional quantities (4) in governing equations (1), (2) gives non-dimensional governing equations (5) and (6)

$$\frac{\partial^2\theta_S}{\partial x^2}+\frac{1}{x}\frac{\partial\theta_S}{\partial x}-\beta=\frac{\partial\theta_S}{\partial Fo},\quad s\leqslant x\leqslant 1 \tag{5}$$

$$\frac{\partial^2\theta_L}{\partial x^2}+\frac{1}{x}\frac{\partial\theta_L}{\partial x}-\beta=\frac{\partial\theta_L}{\partial Fo},\quad 0\leqslant x\leqslant s \tag{6}$$

Similarly the non-dimensional boundary and initial conditions,

(1) $\theta_S(x=1,Fo)=1$.
(2) $\theta_S(x=s,Fo)=0$.
(3) $\theta_L(x=s,Fo)=0$.
(4) $\frac{\partial\theta_L(x=0,Fo)}{\partial x}=0$.
(5) $\theta_L(x,Fo=0)=\frac{T_f-T_i}{T_f-T_0}=\theta_i$.
(6) $s(Fo=0)=1$.

Interface energy equation (3) transforms to,

$$Ste\left(\frac{\partial\theta_S(s,Fo)}{\partial x}-\frac{\partial\theta_L(s,Fo)}{\partial x}\right)=-\frac{\mathrm{d}s}{\mathrm{d}Fo}, \tag{7}$$

where, $Ste$ is the Stefan number defined as, $Ste=\frac{c(T_f-T_0)}{H}$.

Solidification solutions of the above differential equation depend on the dimensionless energy generation parameter $\beta$. It is very difficult to arrive at an exact analytical solution. The transient terms can be neglected by assuming quasi-stationarity. The quasi-steady model is valid for low values of Stefan number. Interface energy equation is unchanged in the model. Hence the interface motion, temperature distribution are time dependent. Since transient terms are negligible, steady state temperature distribution are achieved instantaneously as the interface moves. Neglecting the transient terms, and direct integration of Eqs. (5) and (6) and application of corresponding boundary conditions, gives the solution to the temperature distribution in the solid and liquid phase as,

$$\theta_S(x,Fo)=\frac{\ln x}{4\ln s}(\beta-4-\beta s^2)+\left(1-\frac{\beta}{4}\right)+\frac{\beta}{4}x^2 \tag{8}$$

$$\theta_L(x,Fo)=\frac{\beta}{4}s^2+\frac{\beta}{4}x^2 \tag{9}$$

Differentiating Eqs. (8) and (9), and substituting into interface equation (7), with applying the initial condition $s(Fo=0)=1$, results in

$$Ste\int_0^{Fo}\mathrm{d}Fo=\frac{4}{\beta}\int_1^{S}\frac{s\ln s\,\mathrm{d}s}{s^2+(4/\beta-1)} \tag{10}$$

From Eq. (10), it is clear that the above integral has to be evaluated in three cases ($\beta>4.0$, $\beta<4.0$, $\beta=4.0$).

*2.1.1. Analytical solutions—transient interface position*

Case 1: $\beta<4.0$

$$\begin{aligned}Ste\,Fo=\frac{4}{\beta}\Bigg[&\frac{1}{2}\,\mathrm{dilog}\left(\frac{a_1+si}{a_1}\right)+\frac{1}{2}\,\mathrm{dilog}\left(\frac{a_1-si}{a_1}\right)\\&+\frac{1}{2}\ln s\ln\left(\frac{a_1+si}{a_1}\right)+\frac{1}{2}\ln s\ln\left(\frac{a_1-si}{a_1}\right)\\&-\frac{1}{2}\,\mathrm{dilog}\left(\frac{a_1-i}{a_1}\right)-\frac{1}{2}\,\mathrm{dilog}\left(\frac{a_1+i}{a_1}\right)\Bigg]\end{aligned} \tag{11}$$

where $a_1=\sqrt{4/\beta-1}$, $\mathrm{dilog}(x)$ is a special mathematical function defined by the analytical continuation of the following integral [17].

$\mathrm{dilog}(x) = -\int_0^x \frac{\log(1-t)}{t}\,\mathrm{d}t$ for a real number $x < 1$. These functions are evaluated by using mfun function of MATLAB v7.0 (R14), with an accuracy of $10^{-16}$.

For $\beta < 4$, entire cylinder is solidified at $Fo_{\mathrm{sol}}$, before the steady state is reached. Even after the complete solidification, the temperature of the PCM continues to decrease, because of sensible heat release by the PCM, and its heat generation. Hence the above solution is applicable when $Fo < Fo_{\mathrm{sol}}$. Complete solidification time of cylinders can be calculated by,

$$Ste\,Fo_{\mathrm{sol}} = \frac{4}{\beta}\left[-\frac{1}{2}\,\mathrm{dilog}\left(\frac{a_1 - i}{a_1}\right) - \frac{1}{2}\,\mathrm{dilog}\left(\frac{a_1 + i}{a_1}\right)\right] \quad (12)$$

Case 2: $\beta > 4.0$

$$Ste\,Fo = \frac{4}{\beta}\int_1^S \frac{s\ln s\,\mathrm{d}s}{s^2 - (1 - 4/\beta)}$$

$$\begin{aligned} Ste\,Fo = \frac{4}{\beta}\Bigg[&\frac{1}{2}\,\mathrm{dilog}\left(\frac{a_2 + s}{a_2}\right) + \frac{1}{2}\,\mathrm{dilog}\left(\frac{a_2 - s}{a_2}\right) \\ &+ \frac{1}{2}\ln s\ln\left(\frac{a_2 + s}{a_2}\right) + \frac{1}{2}\ln s\ln\left(\frac{a_2 - s}{a_2}\right) \\ &- \frac{1}{2}\,\mathrm{dilog}\left(\frac{a_2 - 1}{a_2}\right) - \frac{1}{2}\,\mathrm{dilog}\left(\frac{a_2 + 1}{a_2}\right)\Bigg] \end{aligned} \quad (13)$$

where $a_2 = \sqrt{1 - 4/\beta}$.

In this case, cylinder will not completely solidify even when the equilibrium is reached. Instead at steady state, it reaches a particular interface position $s_{ST}$ as defined in (14) at which, all the energy generated is conducted out to the cold water.

$$s_{ST} = \sqrt{1 - \frac{4}{\beta}} \quad (14)$$

Case 3: $\beta = 4.0$

$$Ste\,Fo = \frac{1}{2}(\ln s)^2 \quad (15)$$

This is a very special case, at which the cylinder will completely solidify only when the steady state is reached. At equilibrium state, the interface is at $s = 0$, and all the energy generated is conducted out to the cold surface.

### 2.2. Model II (conduction)

Analytical solutions for finding the transient interface positions is [18],

$$4\,Ste\,Fo = 1 - s^2(1 - 2\ln s) \quad (16)$$

## 3. Melting analysis

The PCM inside the cylinder encapsulation is initially solid at phase change temperature ($T_f$). The surfaces of the cylinder $\xi = \pm R$ are maintained at a temperature $T_0 > T_f$. Melting of PCM starts from the surface and the interface moves inward. Due to the temperature rise and presence of heat generation, solid phase will result in partial melting and hence solid–liquid region is formed instead of solid phase. Since quasi-steady approximation method is used, it is assumed that the mixture forms immediately and the temperature of the solid phase rises instantaneously to the fusion temperature. Temperature of the mixture will be at its fusion temperature. But the proportion of liquid in the mixture increases due to energy generation, and sensible heat addition from the warm surface. Once the entire cylinder melts, liquid temperature will rise until steady state is reached.

### 3.1. Model I (conduction and heat generation)

In the dimensionless formulation, the energy generation parameter $\beta$, Stefan number $Ste$ and dimensionless temperature $\theta_L$ are redefined as,

$$\beta = \frac{R^2 q'''}{k(T_0 - T_f)}, \quad Ste = \frac{c(T_0 - T_f)}{H}$$

$$\theta_L = \frac{T_0 - T(\xi, t)}{T_0 - T_f} \quad (17)$$

Transient heat equation with energy generation for the liquid phase is,

$$\alpha\left(\frac{\partial^2 T_L}{\partial \xi^2} + \frac{1}{\xi}\frac{\partial T_L}{\partial \xi}\right) + \frac{q'''}{\rho c} = \frac{\partial T_L}{\partial t} \quad (18)$$

where $\alpha$—thermal diffusivity of PCM.

The boundary conditions and initial condition includes,

(1) $T_L(\xi = R, t) = T_0$.
(2) $T_L(\xi = \sigma, t) = T_f$.
(3) $\sigma(t = 0) = R$.

Dimensionless heat equation, boundary and initial conditions are,

$$\frac{\partial^2 \theta_L}{\partial \xi^2} + \frac{1}{x}\frac{\partial \theta_L}{\partial x} - \beta = \frac{\partial \theta_L}{\partial Fo}, \quad s \leqslant x \leqslant 1 \quad (19)$$

$$\theta_L(x = 1, Fo) = 0$$

$$\theta_L(x = s, Fo) = 1$$

$$s(Fo = 0) = 1$$

Assuming quasi-stationarity, transient terms from the governing equation can be neglected and solving the differential equation, yields,

$$\theta_L(x, Fo) = \frac{\ln x}{\ln s}\left(1 + \frac{\beta}{4} - \frac{\beta}{4}s^2\right) - \frac{\beta}{4} + \frac{\beta}{4}x^2 \quad (20)$$

As explained a mixture of solid and liquid phases are formed during melting instead of solid phase because of partial melting. Hence the interface energy equation is reformulated with an addition of a factor $\gamma$ which defines the mass proportion of liquid in the mixture.

The conservation of energy for the mixture is represented in Eq. (21)

$$q''' = \rho H\frac{\mathrm{d}\gamma}{\mathrm{d}t} \quad (21)$$

Integrating the above equation and using the initial condition $\gamma(0) = 0$

$$\gamma = \frac{q'''}{\rho H} t \tag{22}$$

Assuming, no heat is transferred through the mixture by conduction and from Eq. (22), the interface energy equation is modified into,

$$-k \frac{\partial T_L(\xi = \sigma, t)}{\partial \xi} = \rho H (1 - \gamma) \frac{\mathrm{d}\sigma}{\mathrm{d}t} \tag{23}$$

where $\gamma$ is the mass ratio of liquid in the mixture to the total mass of mixture.

Dimensionless interface energy equation is,

$$Ste \left. \frac{\partial \theta_L}{\partial x} \right|_{x=s} = (1 - Ste\, Fo\, \beta) \frac{\mathrm{d}s}{\mathrm{d}Fo} \tag{24}$$

Resorting to the analytical solution (20),

$$\left. \frac{\partial \theta_L}{\partial x} \right|_{x=s} = \frac{4 + \beta - \beta s^2}{4 s \ln s} + \frac{\beta}{2} s \tag{25}$$

Substituting (25) in (24) yields,

$$4 = (4 + \beta - \beta s^2 + 2\beta s^2 \ln s)(1 - Ste\, Fo\, \beta) \tag{26}$$

Complete melting time of the cylinder can be computed by [i.e. $s = 0$, $Fo = Fo_{\mathrm{mel}}$],

$$Ste\, Fo_{\mathrm{mel}} = \frac{1}{\beta + 4} \tag{27}$$

### 3.2. Model II (conduction)

Limiting case of $\beta = 0$, results in

$$Fo_{\mathrm{mel}} = \frac{1}{4} Ste^{-1} \tag{28}$$

It is evident from the two equations (27) and (28); the presence of energy generation reduces total melting time.

### 3.3. Model III (conduction, convection and heat generation)

During melting, as the melted region grows, the influence of natural convection has a considerable impact. As proposed [19] the natural convection effect of PCM can be merged with the thermal conductivity of the liquid by using a relation (29),

$$\lambda_{\mathrm{leq}}(t) = k_{\mathrm{eq}}(t) * k \tag{29}$$

where

- $k$ is thermal conductivity of PCM.
- $k_{\mathrm{eq}}(t)$—ratio of transferred heat rate by natural convection to that by thermal conduction.
- $\lambda_{\mathrm{leq}}(t)$—equivalent thermal conductivity of the liquid PCM.
- Overall equivalent conductivity

  $k_{\mathrm{eq}}(t) = Nu/Nu_{\mathrm{cond}}$
- Overall Nusselt number is given by,

  $Nu = [Nu_{\mathrm{cond}}^{15} + Nu_{\mathrm{conv}}^{15}]^{(1/15)}$

  where

$$Nu_{\mathrm{cond}} = \frac{2}{\ln(R/\sigma)}$$

$$Nu_{\mathrm{conv}} = \left[ \frac{1}{Nu_\sigma} + \frac{1}{Nu_R} \right]^{-1}$$

The non-dimensional analytical solutions given are same for models I and III. But for model III, at each time step the equivalent thermal conductivity $\lambda_{\mathrm{leq}}(t)$ has to be calculated. This equivalent thermal conductivity $\lambda_{\mathrm{leq}}(t)$ is substituted instead of the conductivity $k$.

## 4. Experimental setup and test procedure

The experiments consists of two insulated section namely test tank and auxiliary unit. At the centre of the tank a cylinder is filled with PCM as shown in Fig. 2. The auxiliary unit is provided with a heating coil and a cooling coil in order to heat or cool the circulating fluid based on the condition required. The water with additive ethylene glycol (73:27 % by wt) is used as circulation fluid. The temperature of the fluid can be varied between −25 to 50 °C. Constant wall temperature of the cylinder can be maintained during the experiment through the circulation of the external fluid from the constant temperature bath. Temperature controller with electrical stirrer is used to maintain the uniformity of the temperature inside the tank and the bath. The estimated uncertainty in the temperature measurement is ±1.8 °C and the resolution of digital temperature controller is 0.1 °C. Initially both temperature controllers (tank, bath) are set at the same temperature. Also thermocouples are evenly spaced and fixed at the external surface of the PCM at several locations to check the uniformity of the temperature boundary condition. These thermocouples are connected to the temperature controller. This ensures uniform surface temperature at the beginning of the test within 0.5 °C. The storage capsule is a copper capsule with inner diameter of 70 and 350 mm long with a wall thickness of 1 mm. Digital camera is used to record the solidification and melting images at various stages of the process. Refractive index of the external fluid is found to be 1.36 whereas refractive index of the HC mixture is 1.434 which is comparable. Even then slight distortion effects will be present due to the refraction. Transient interface positions are measured by digital image processing methods such as contrast enhancement, and filtering operations which minimizes the uncertainties in the position measurements. PCM chosen for the experiment is a 60% $n$-tetradecane + 40% $n$-hexadecane mixture, claimed to be suitable for cool thermal energy storage. Since HC mixture contains air particles, during preparation of sample air particles are removed by repeating solidification and melting under vacuum. Some properties of HC mixture chosen are taken from literature while others are determined by DSC measurements. The top and bottom of the test tank were fitted with double glazed plexiglass windows to enable photographic and visual observations of the test cylinder. For solidification, only 76% of the liquid PCM is filled inside the test cylinder. An overflow tube is provided at the top in order to remove the excessive PCM during filling. During the test, the phase change process is monitored and the light projector was switched on.

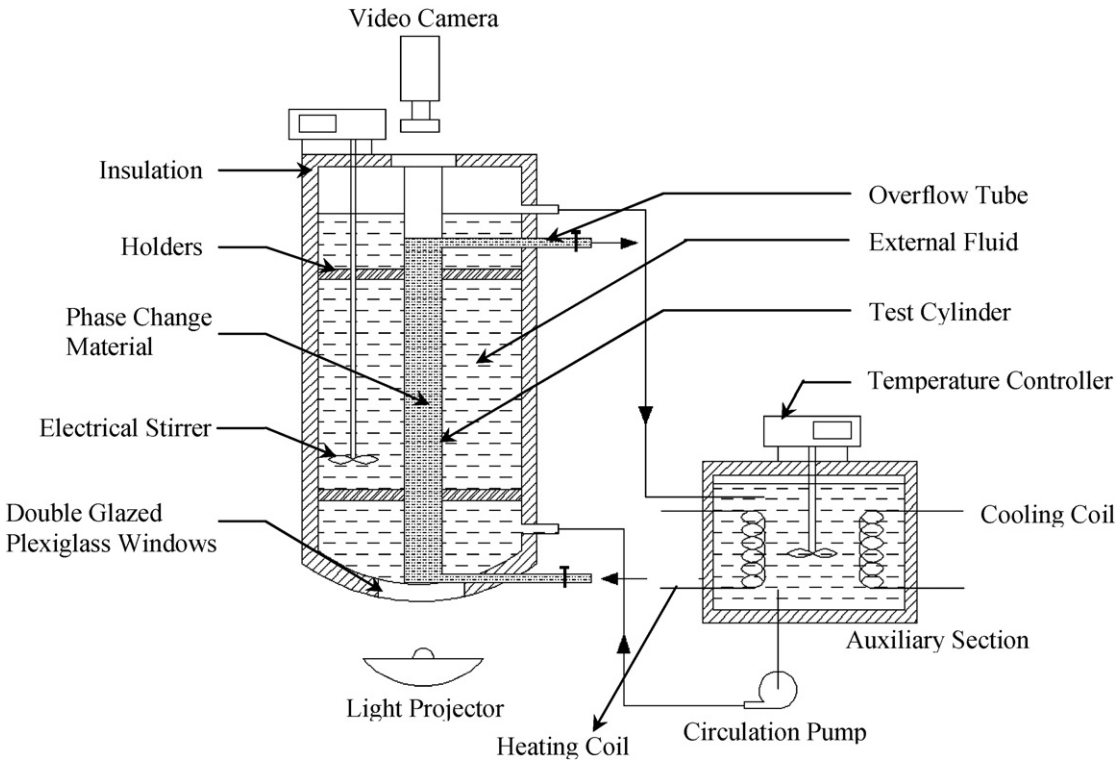


Fig. 2. Experimental setup.

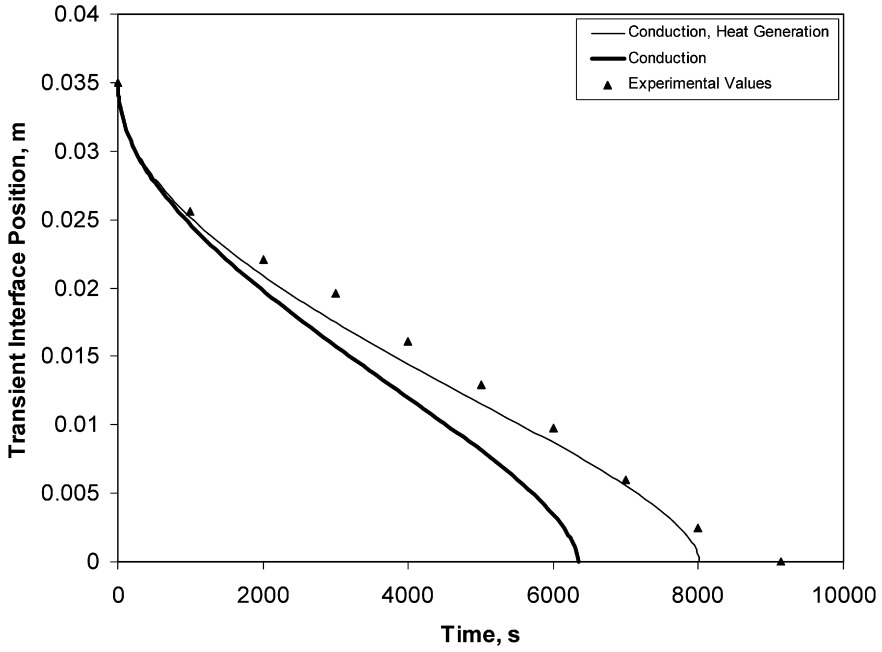


Fig. 3. Comparison between experimental study and analytical solutions (solidification, radius of the cylindrical capsule = 35 mm, external fluid temperature = −8 °C).

## 5. Results and discussion

### 5.1. Solidification

#### 5.1.1. Experimental validation

Experimentations were conducted using HC mixture (60% *n*-tetradecane + 40% *n*-hexadecane) with external fluid temperature of −8 °C. To determine the solidification front, periodically the digital images of the test cylinder were extracted. Thus obtained results are compared with the analytical solution and it is shown in Fig. 3. Analytically, transient interface positions and complete solidification time is predicted by two models. Model I involves conduction and energy generation, whereas model II is a pure conduction model. The time for complete

solidification predicted from conduction model (model II) is 30% lower than the experimental results. But the time predicted by the model I is about 11% lower than experimentally measured values. The agreement between experimental and analytical values is quite good for lower values of non-dimensional parameter (*Ste Fo*).

*5.1.2. Analytical solution*

Having validated the conduction and heat generation model, the same model is extended to study the heat transfer characteristics and phase change behavior of PCM inside the containment. The transient solid and liquid temperature profiles for various values of $\beta$ are shown in Fig. 4. Low-dimensionless heat

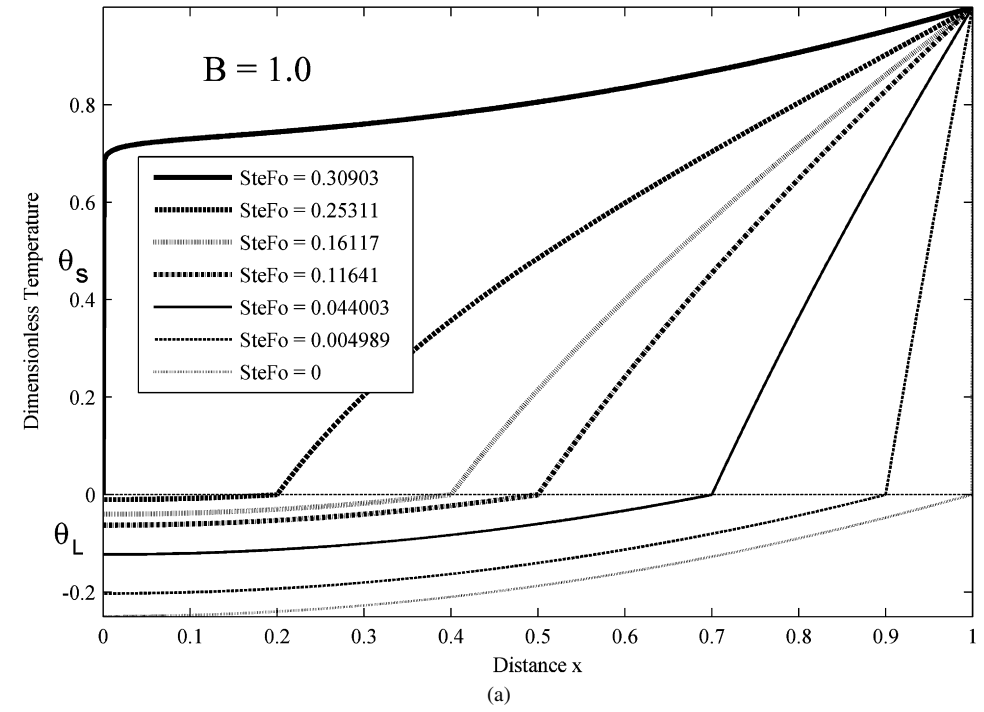


(a)

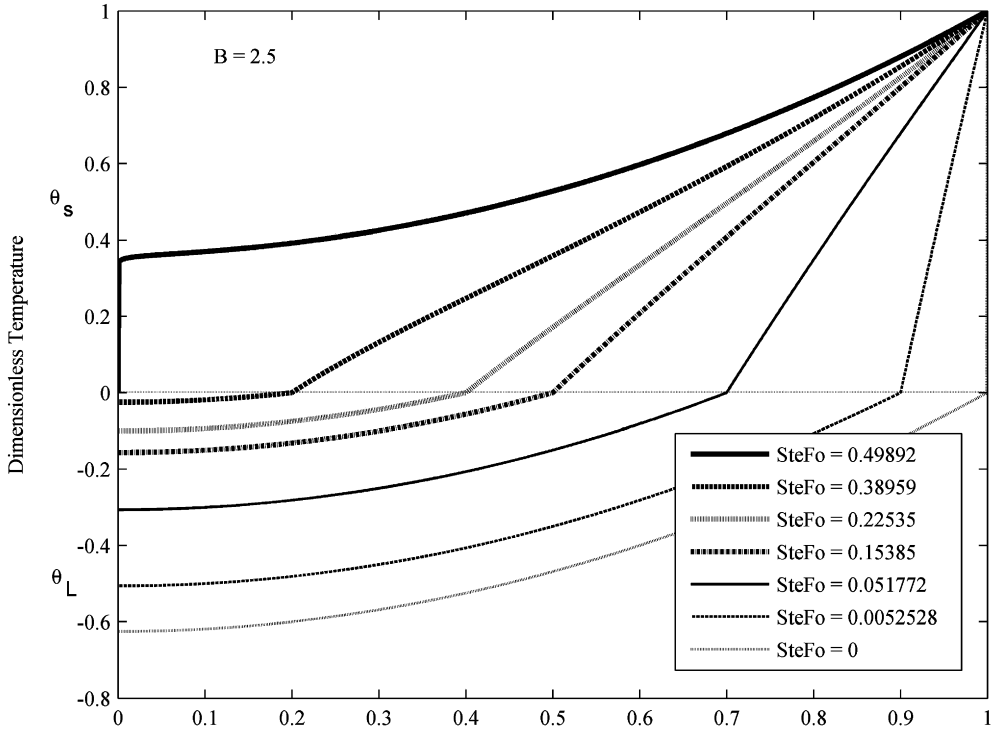


(b)

Fig. 4. (a) Transient temperature profiles (solidification) $\beta = 1.0$. (b) Transient temperature profiles (solidification) $\beta = 2.5$. (c) Transient temperature profiles (solidification) $\beta = 4.0$. (d) Transient temperature profiles (solidification) $\beta = 6.0$.

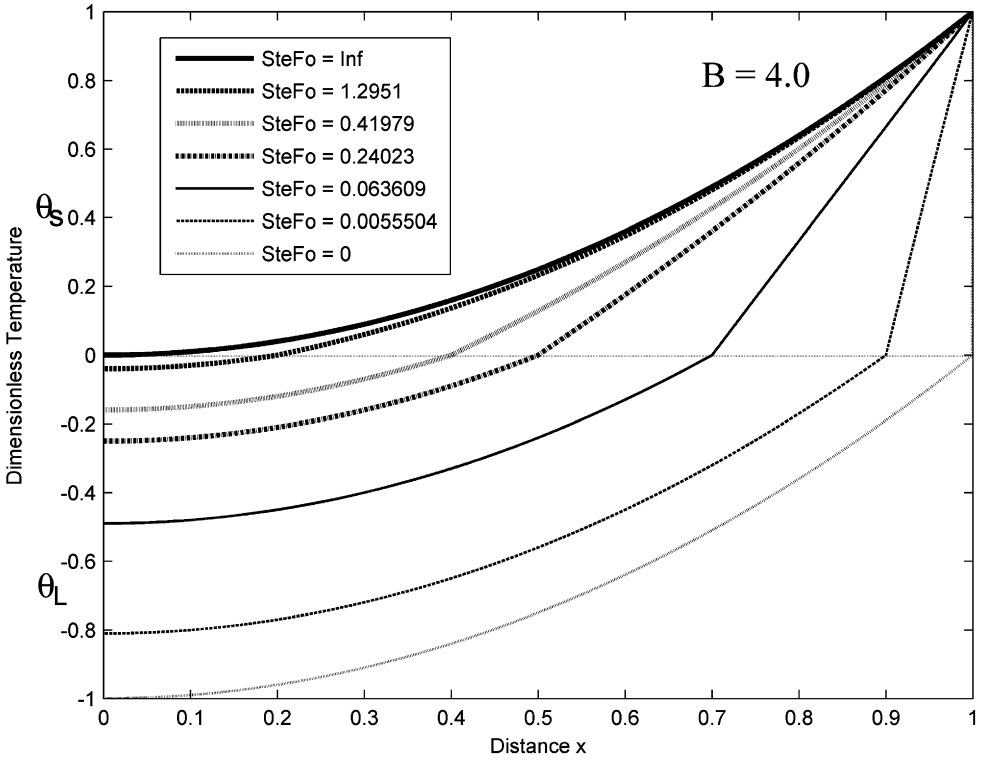


(c)

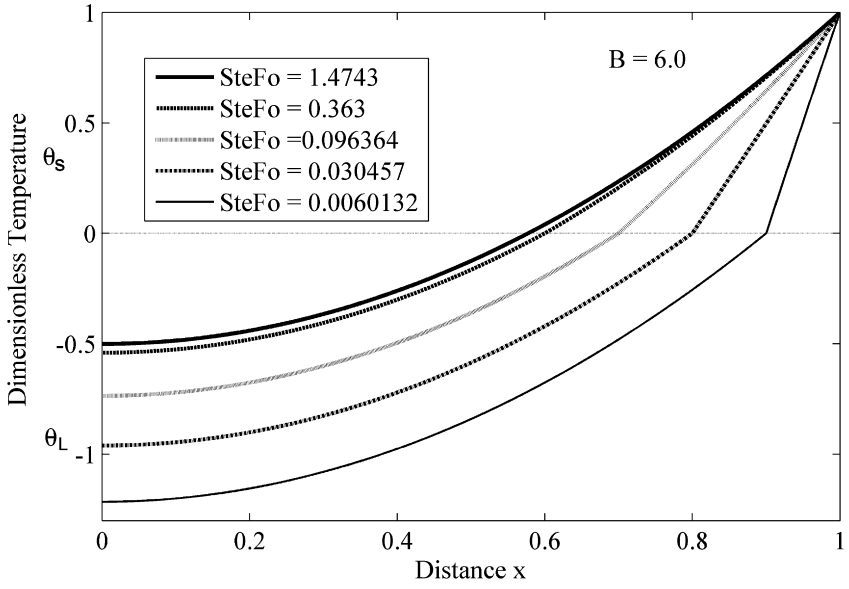


(d)

Fig. 4. (*Continued*.)

generation ($\beta$) will have lower solid phase temperatures ($T_S$). This shows that lower $\beta$ terms, will have faster solidification. Similarly, it is evident that higher *Ste* values will have rapid solidifying rates. Since quasi-steady condition is assumed, as expected variations in temperature in the liquid phase are observed. Discontinuities in the temperature gradient at the interface at lower $\beta$ values can be found. But these discontinuities almost disappear when $\beta > 4.0$ for cylinder.

The effect of heat generation parameter on transient interface positions is shown in Fig. 5. Heat generation slows down the motion of the interface, because high heat generation requires higher heat extraction from the surface, in order to have a growth in the solidification layer. For higher heat generation values $\beta > 4.0$, steady state is reached, even without total solidification. Where as for low heat generation $\beta < 4.0$, total solidification takes place without reaching steady state. The unique case of $\beta = 4.0$, total solidification will takes place at the steady state, but for slab it is at $\beta = 2.0$ [1]. The effect of heat generation on percentage solidification is represented in Fig. 6. For thermal energy storage (TES) applications, it can be

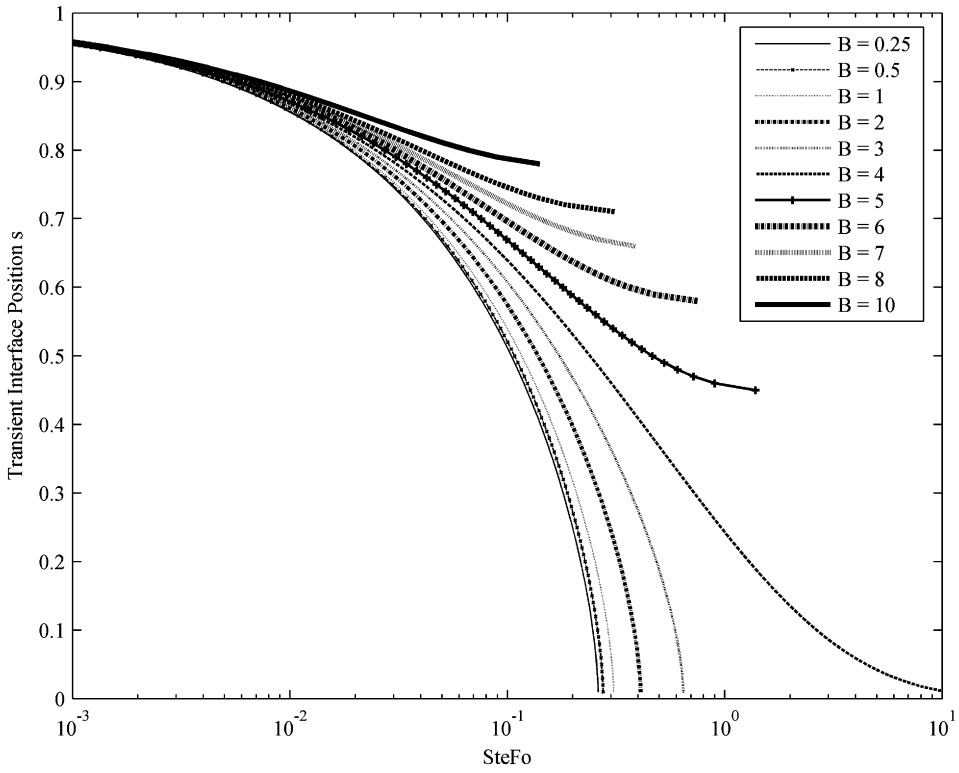


Fig. 5. Transient interface positions for various heat generation parameter $\beta$ (solidification).

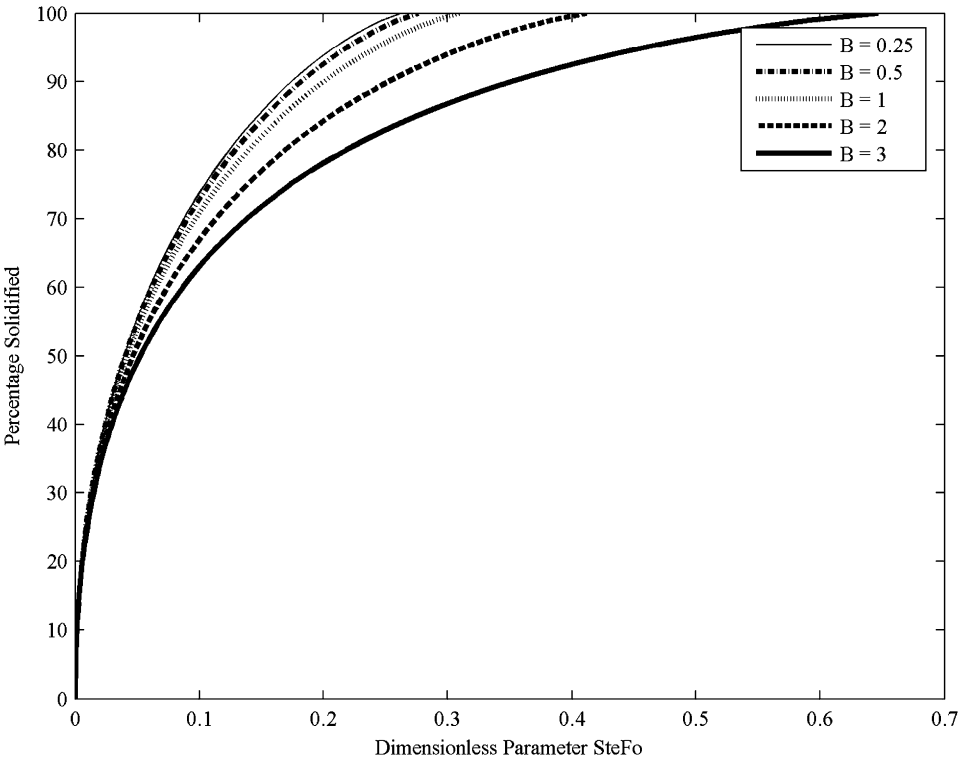


Fig. 6. Effect of heat generation on percentage solidification.

inferred that TES storage can be solidified approximately 80% instead of complete solidification. Since thermal energy storage should always be characterized by rapid charging and discharging rates. Fig. 7 shows steady state interface position for various heat generation $\beta$. The steady state percentage solidification of the PCM decreases as $\beta$ increases.

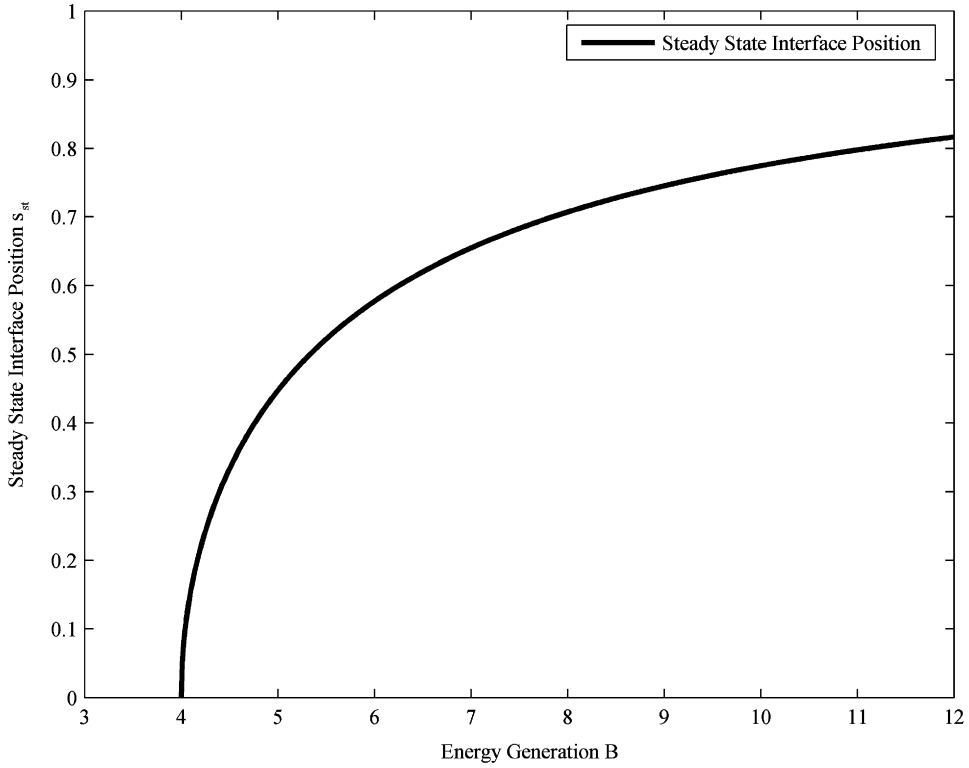


Fig. 7. Steady state interface positions (solidification).

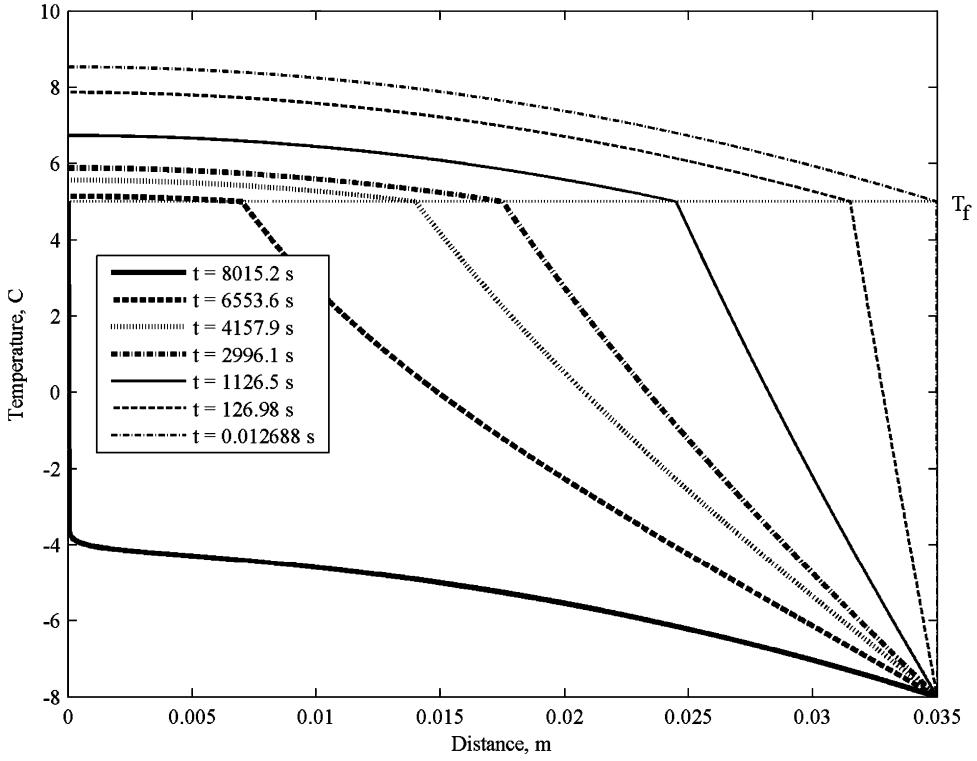


Fig. 8. Transient temperature profiles for 60% *n*-tetradecane + 40% *n*-hexadecane (solidification, radius of the capsule = 35 mm, external fluid temperature = −8 °C).

### *5.1.3. Application*

Transient temperature profile for the chosen mixture is represented in Fig. 8. The influence of external fluid temperature and radius of the capsule on total solidification time is presented in Fig. 9. It shows that smaller capsules will solidify quickly, since heat has to travel only smaller distance and hence charging rate will be higher for smaller capsules. It is also noted that for lower external fluid temperature, rapid

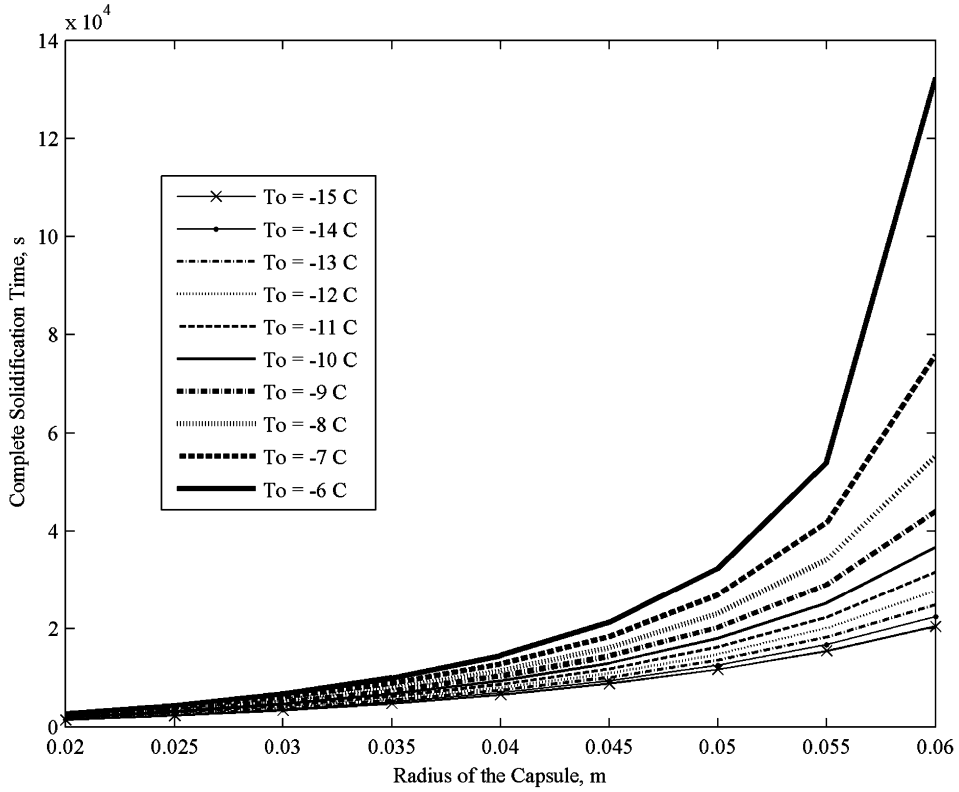


Fig. 9. Influence of external fluid temperature and radius of the capsule on total solidification time for 60% $n$-tetradecane + 40% $n$-hexadecane.

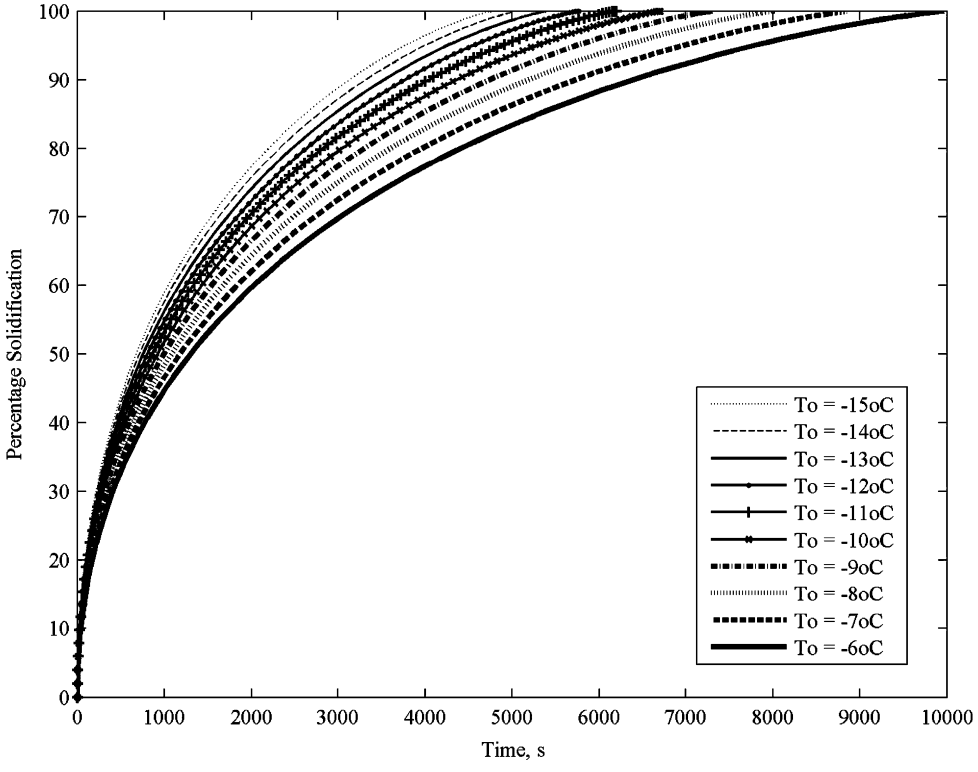


Fig. 10. Influence of external fluid temperature on percentage solidification (radius of the capsule = 35 mm).

charging takes place resulting in faster solidification. Hence complete solidification time is lower for higher Stefan numbers (or lower heat transfer fluid temperature).This fact is more precisely given in Fig. 10. It shows that higher heat transfer fluid temperature will have low percentage of solidification.

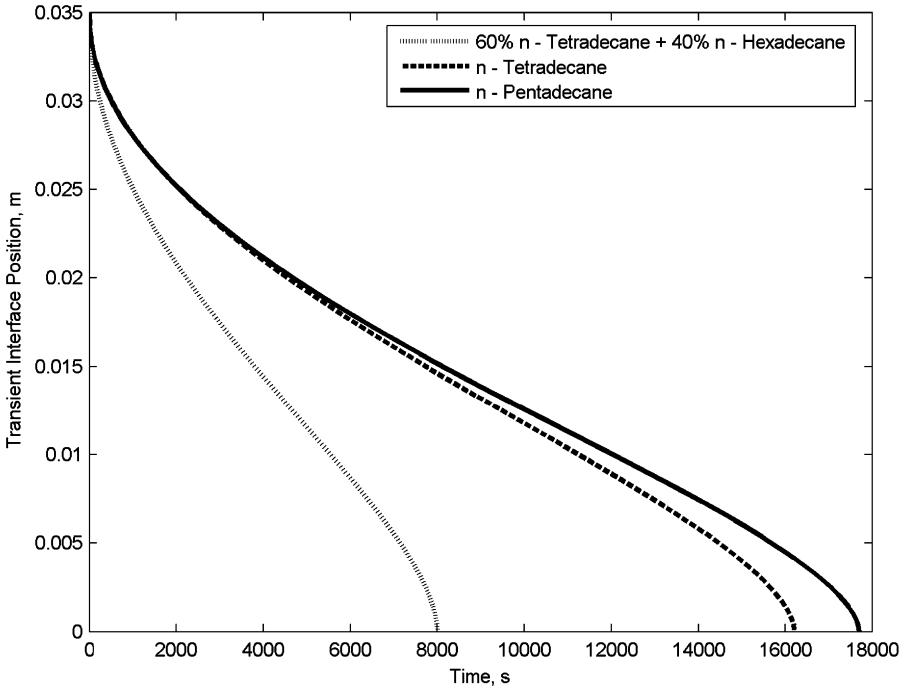


Fig. 11. Solidification characteristics of the PCMs (60% *n*-tetradecane + 40% *n*-hexadecane, *n*-tetradecane, and *n*-pentadecane, radius of the capsule = 35 mm, external fluid temperature = −8 °C).

Table 1
Thermo-physical properties of the PCM

| Properties | *n*-tetradecane : *n*-hexadecane (6 : 4) | *n*-tetradecane | *n*-pentadecane |
|---|---|---|---|
| Melting point, °C | 5.0 | 5.5 | 9.6 |
| Latent heat of melting, kJ/kg | 121.8 | 227 | 168 |
| Specific heat of liquid, kJ/kg K | 2.13 | 2.16 | 3.53 |
| Specific heat of solid, kJ/kg K | 1.64 | 1.64 | 3.08 |
| Thermal conductivity of liquid, W/mK | 0.146 | 0.15 | 0.15 |
| Thermal conductivity of solid, W/mK | 0.34 | 0.35 | 0.182 |
| Dynamic viscosity, Pa S | 0.0023 | 0.0023 | 0.00262 |
| Density of liquid, kg/m$^3$ | 765 | 759 | 727.2 |
| Density of solid, kg/m$^3$ | 795 | 884 | 776.1 |

#### *5.1.4. Comparisons*

Validated analytical solution is used to study the behavior of PCMs 60% *n*-tetradecane + 40% *n*-hexadecane, *n*-tetradecane, and *n*-pentadecane. Transient interface plots for corresponding PCMs are presented in Fig. 11. The properties of the PCMs are given in Table 1. The 60% *n*-tetradecane + 40% *n*-hexadecane mixture solidifies faster than the other two materials. *n*-pentadecane and *n*-tetradecane requires double the time to solidify than the chosen mixture. Total solidification time of cylinder for the selected mixture is 8015 s. Hence PCM 1 can be a suitable candidate for cool thermal storage since it has a rapid charging rate.

### *5.2. Melting*

#### *5.2.1. Experimental validation*

Melting front position comparisons for derived analytical models and experimental results have been shown in Fig. 12. Melting characteristics are analyzed by three analytical models. Model I consists of conduction and energy generation; model II represents a pure conduction model and model III includes conduction, convection and heat generation. A comparison of analytical solutions with experimental results shows that model III is good in predicting front positions. Initially the experimental values closely match with the model I, because at the beginning the conduction is the dominant mode of heat transfer. After that, melting is also influenced by natural convection phenomena. Pure conduction model over predicts the complete melting time. Model I predicts total melting time 47.59% higher than the experimental values. But complete melting time predicted by model III, is only 16.11% higher than experimentally observed values. Hence, it is clear that melting process involves natural convection effect in liquid phase. Analytical solution presented for model III, is quite good in predicting the positions at lower *Fo* values.

#### *5.2.2. Analytical solution*

Melting is characterized by a pure liquid phase and a solid–liquid mixture at the fusion temperature. Transient temperature

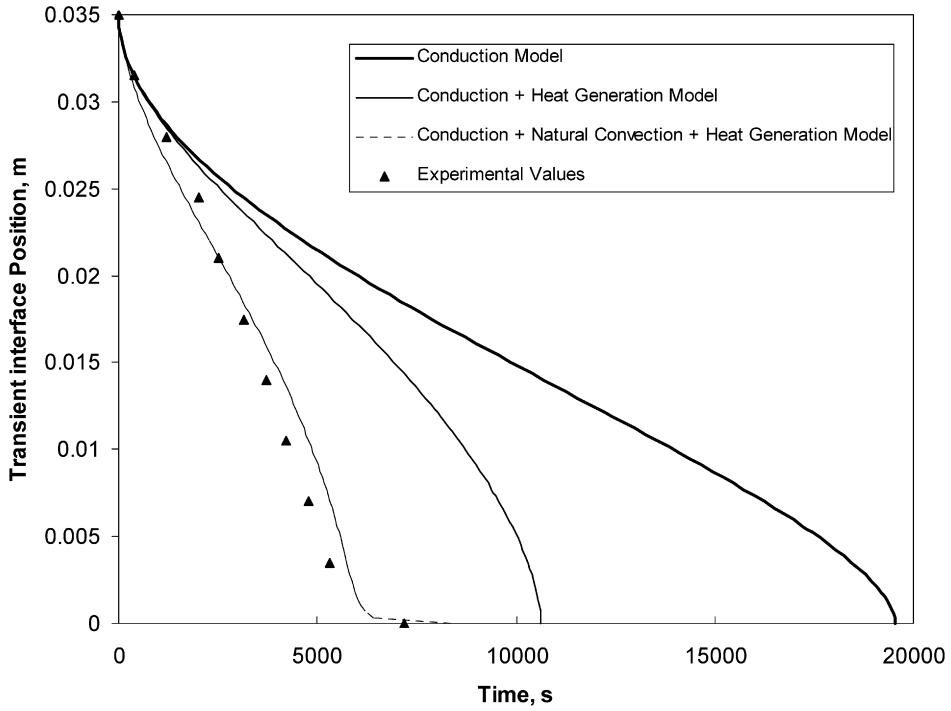


Fig. 12. Comparison between experimental study and analytical solutions (melting, radius of the capsule = 35 mm, external fluid temperature = 15 °C).

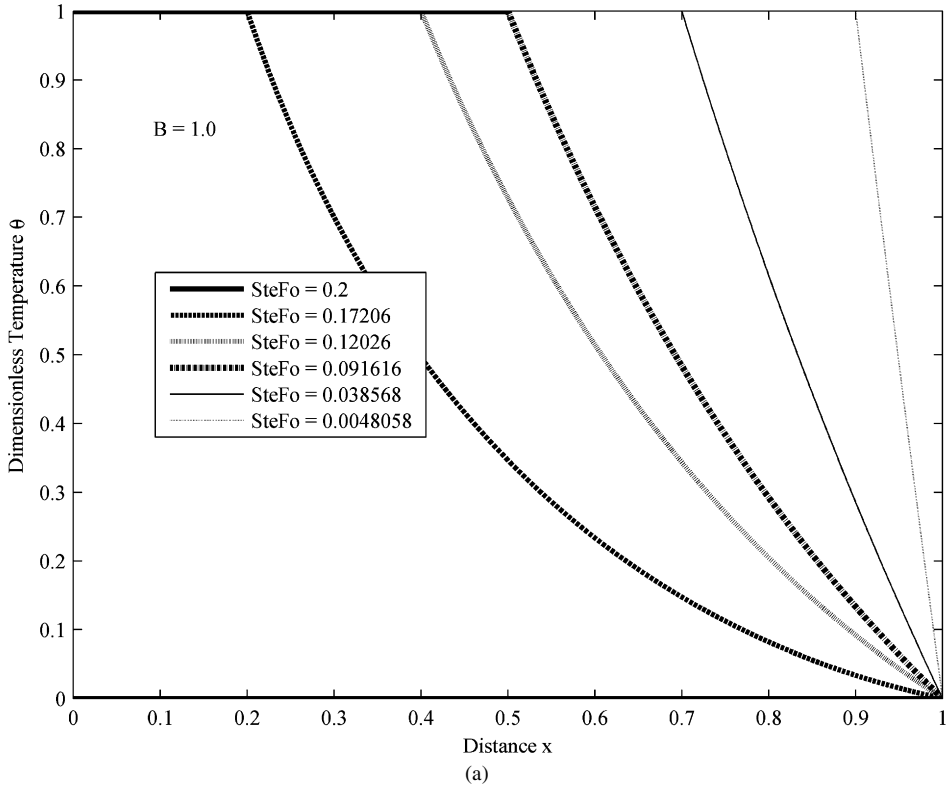


(a)

Fig. 13. (a) Transient temperature profiles (melting) $\beta = 1.0$. (b) Transient temperature profiles (melting) $\beta = 2.5$. (c) Transient temperature profiles (melting) $\beta = 5.0$.

profiles of liquid PCM for various values of $\beta$ is given in Fig. 13. Some times due to high heat generation, the temperature inside the liquid PCM will be higher when compared with warm surface. Hence it has negative values of $\theta_L$. Similar to solidification, higher Stefan number characterizes rapid melting. Fig. 14 shows transient interface positions for various dimensionless time steps. Unlike solidification, higher heat generation shortens melting time. Complete melting time for various values of $\beta$ is illustrated in Fig. 15. It is observed that the presence of heat generation reduces total melting time significantly. The

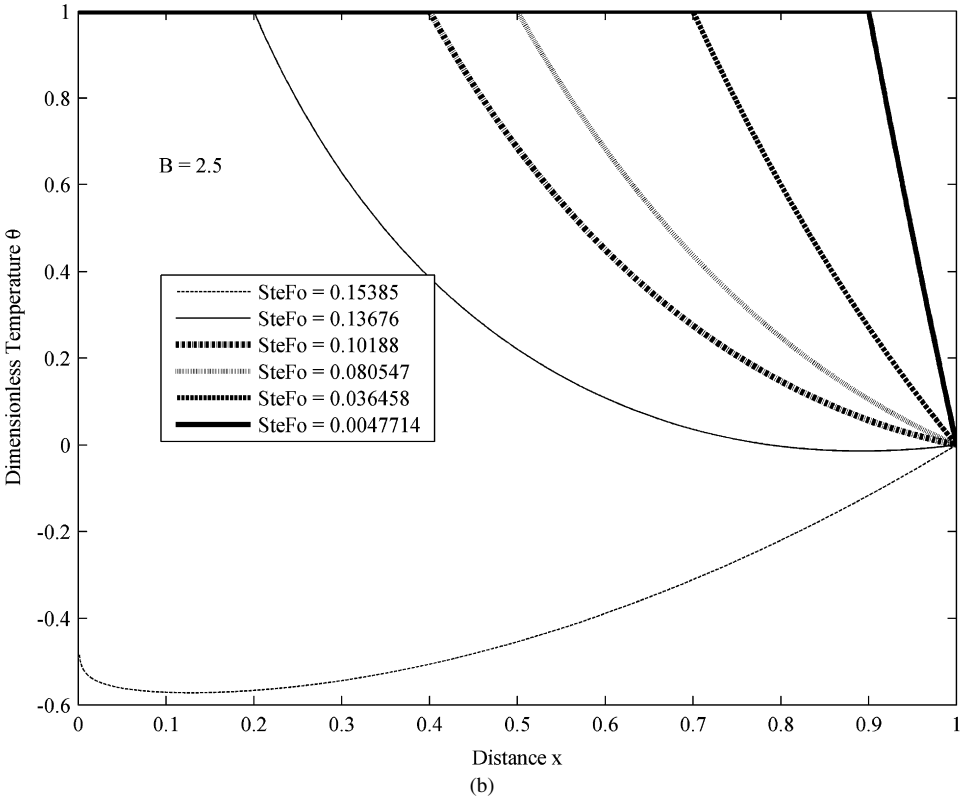


(b)

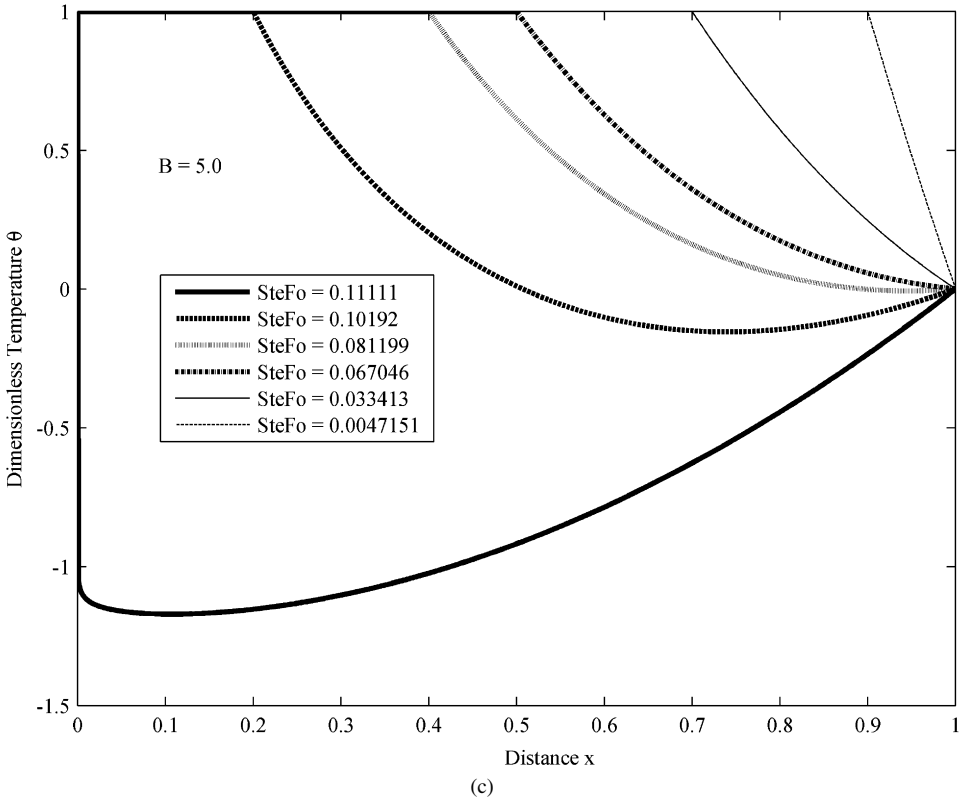


(c)

Fig. 13. (*Continued*.)

validated analytical model is used to study the behavior of PCM inside cylindrical capsule. Transient temperature profiles of the PCM 60% *n*-tetradecane and 40% *n*-pentadecane is given in Fig. 16.

### 5.2.3. *Comparisons*

Melting characteristics of the PCMs are compared in Fig. 17. The discharge characteristics of *n*-tetradecane and *n*-pentadecane show that melting rate of *n*-tetradecane is initially higher,

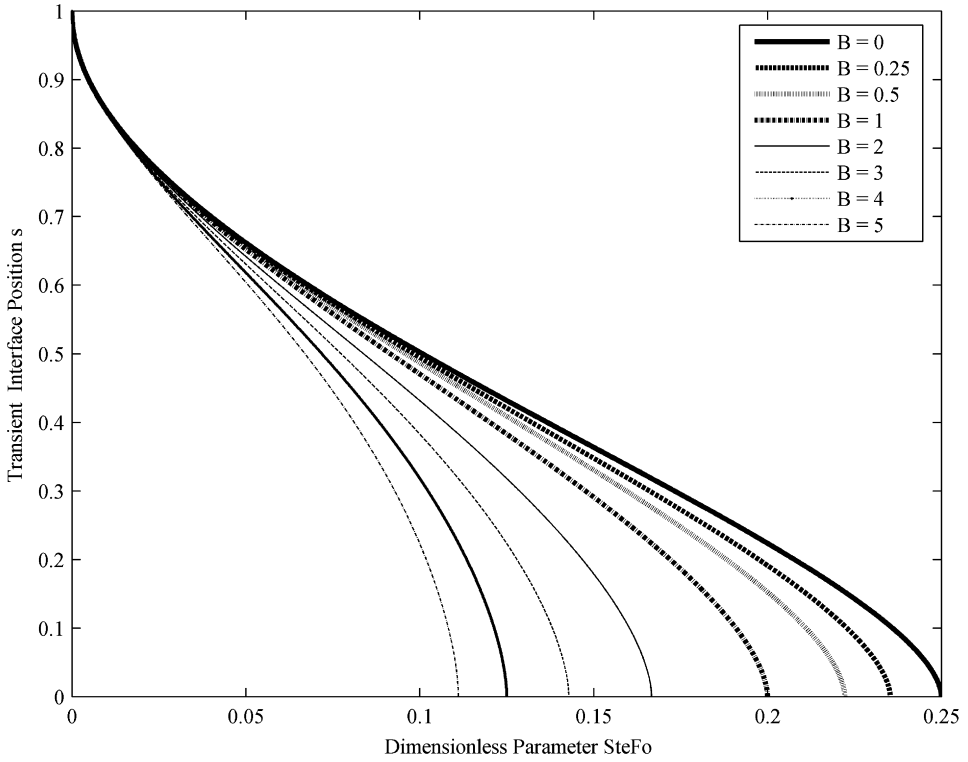


Fig. 14. Transient interface positions (melting).

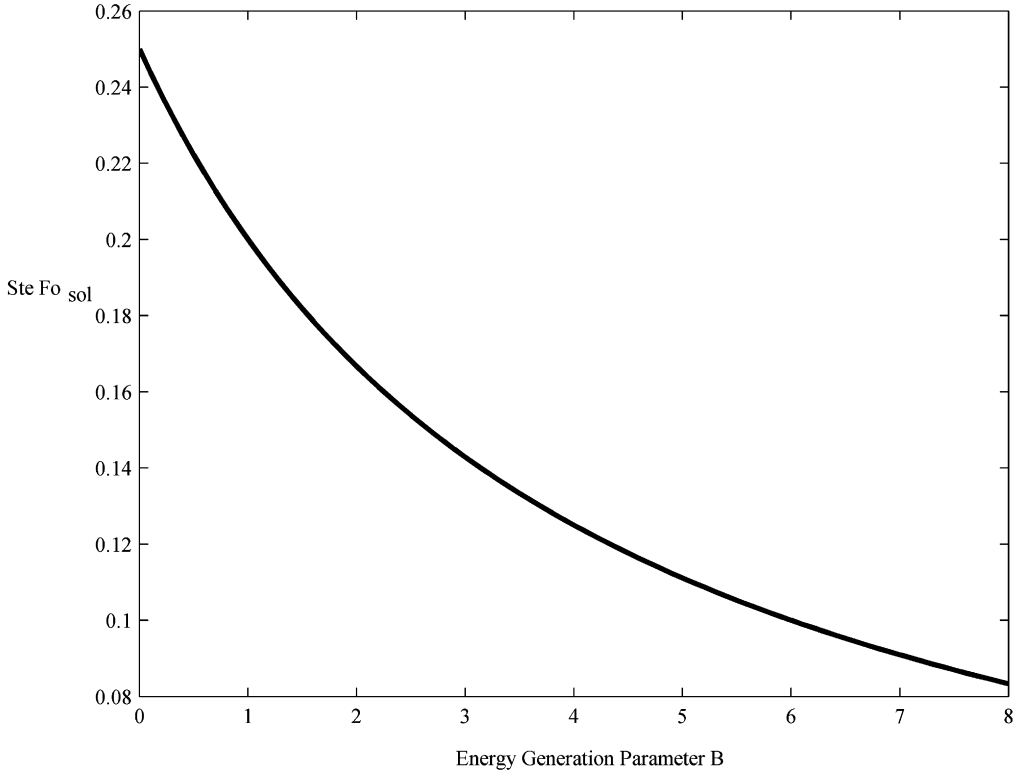


Fig. 15. Total melting time for various heat generation parameter $\beta$.

but $n$-pentadecane melts faster. 60% $n$-tetradecane + 40% $n$-hexadecane melts very quickly when compared with the other two PCMs. So the chosen PCM also have excellent melting characteristics.

## 6. Conclusion

Solidification and melting characteristics of PCMs encapsulated inside cylinders are analyzed based on the obtained

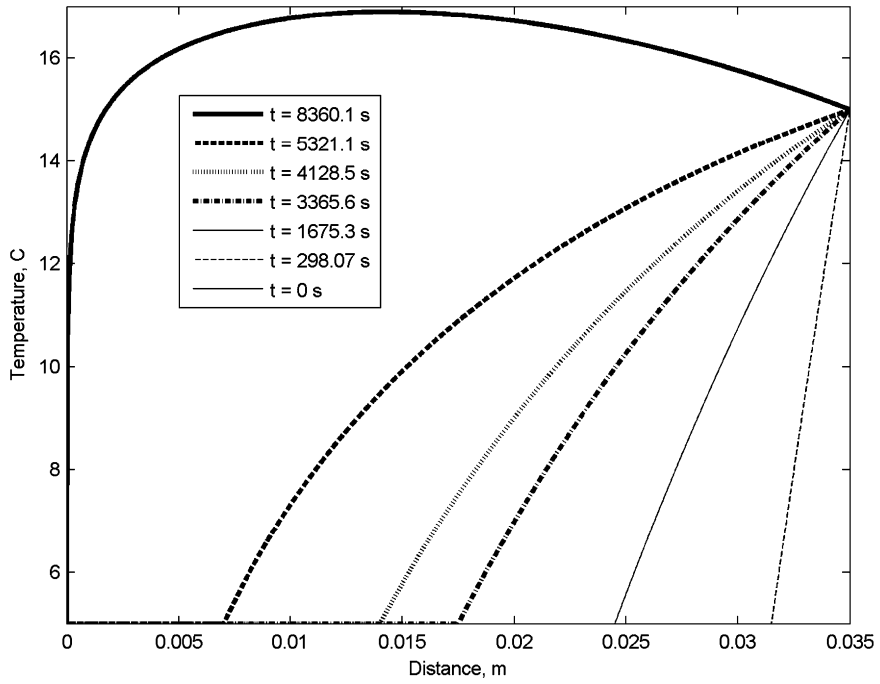


Fig. 16. Transient temperature profiles for 60% $n$-tetradecane + 40% $n$-hexadecane (melting, radius of the capsule = 35 mm, external fluid temperature = 15 °C).

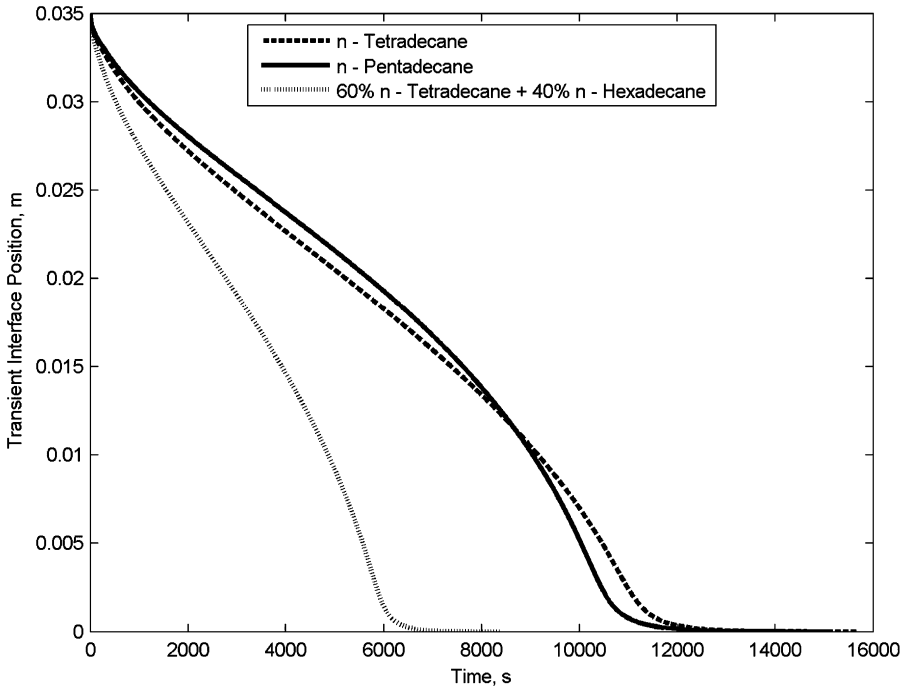


Fig. 17. Melting characteristics of the PCMs (60% $n$-tetradecane + 40% $n$-hexadecane, $n$-tetradecane, and $n$-pentadecane, radius of the capsule = 35 mm, external fluid temperature = 15 °C).

analytical models. Front positions are compared for derived analytical models with experimental values. For solidification, the analytical model with conduction and heat generation is good in predicting interface positions. The analytical result is 11% lower than experimentally measured values. Melting process is initially dominated by conduction and later characterized by natural convection. Deviations between analytical and experimental results are 16.11%. Total solidification time depends on parameters like Stefan number (*Ste*) and heat generation parameter ($\beta$), however total melting time also depends on equivalent thermal conductivity ($\lambda_{\mathrm{leq}}(t)$).

For higher heat generation values $\beta > 4.0$, steady state is reached, even without total solidification, where as for low heat generation $\beta < 4.0$, total solidification takes place without reaching steady state. The unique case of $\beta = 4.0$, total solidification will takes place at the steady state. However, melting

is characterized by the absence of steady state condition prior to total melting of cylinder. Higher Stefan number characterizes rapid solidifying and melting rates. But, presence of heat generation, delays the solidification, whereas it accelerate melting. During solidification, heat generation slows down the motion of the interface. Influence of size of the cylinder, and external fluid temperatures are also investigated. The tetradecane–hexadecane (6:4) mixture solidifies at 8015 s whereas the other two PCMs *n*-tetradecane, *n*-pentadecane solidifies at 16 220 s, 17 700 s respectively. The HC mixture also shows excellent melting characteristics.

## References

[1] L.M. Jiji, S. Gaye, Analysis of solidification and melting of PCM with energy generation, Applied Thermal Engineering 26 (2006) 568–575.
[2] J.F. Li, L. Li, F.H. Stott, Comparison of volumetric and surface heating sources in the modeling of laser melting of ceramic materials, International Journal of Heat and Mass Transfer 47 (2004) 1159–1174.
[3] J.F. Nastaj, A parabolic cylindrical Stefan problem in vacuum freeze drying of random solids, International Communications in Heat and Mass Transfer 30 (1) (2003) 93–104.
[4] P. Rattanadecho, Theoretical and experimental investigation of microwave thawing of frozen layer using a microwave oven (effects of layered configurations and thickness), International Journal of Heat and Mass Transfer 47 (2004) 937–945.
[5] T. Basak, Analysis of resonances during microwave thawing of slabs, International Journal of Heat and Mass Transfer 46 (2003) 4279–4301.
[6] M. El-Genk, W. Cronenberg, An assessment of fuel freezing and drainage phenomena in a reactor shield plug following a core disruptive accident, Nuclear Engineering and Design 47 (1978) 195–225.
[7] W.L. Chen, M. Ishii, M.A. Grolmes, An application of the simple fuel pin transient and melting model for thermal-hydraulics in LMFB assembly, Nuclear Engineering and Design 53 (1979) 321–338.
[8] K.A.R. Ismail, J.R. Henrıquez, Numerical and experimental study of spherical capsules packed bed latent heat storage system, Applied Thermal Engineering 22 (2002) 1705–1716, 1707.
[9] N. Shamsundar, E.M. Sparrow, Analysis of multidimensional conduction phase change via the enthalpy model, Journal of Heat Transfer, Transactions of the ASME (August 1975) 333–340.
[10] N. Shamsundar, E.M. Sparrow, Effect of density change on multidimensional conduction phase change, Journal of Heat Transfer, Transactions of the ASME 98 (1976) 550–557.
[11] R.M. Furzerland, A comparative study of numerical methods for moving boundary problems, Journal of the Institute of Mathematics and Its Applications 26 (1980) 411–429.
[12] S. Savovic, J. Caldwell, Finite difference solution of one-dimensional Stefan problem with periodic boundary conditions, International Journal of Heat and Mass Transfer 46 (15) (2003) 2911–2916.
[13] A.I. Fedorchenko, A.A. Chernov, Exact solution of the problem of gas segregation in the process of crystallization, International Journal of Heat and Mass Transfer 46 (5) (2003) 915–919.
[14] M. Farid, The moving boundary problems from melting and freezing to drying and frying of food, Chemical Engineering and Processing 41 (2002) 1–10.
[15] P. Lamberg, Approximate analytical model for two-phase solidification problem in a finned phase-change material storage, Applied Energy 77 (2004) 131–152.
[16] A. Siahpush, J. Crepeau, Integral solutions of phase change with internal heat generation, in: Proc. of 12th Int. Conf. on Nucl. Eng., April 25–29, 2004, Arlington, VA, 2004.
[17] J. Murakami, A. Ushijima, A volume formula for hyperbolic tetrahedral in terms of edge lengths, math.MG/0402087 (12 pp.).
[18] A. Barba, M. Spiga, Discharge mode for encapsulated PCMs in storage tanks, Solar Energy 74 (2003) 141–148.
[19] T. Hirata, K. Nishida, An analysis of heat transfer using thermal conductivity of liquid phase during melting inside an isothermally heated horizontal cylinder, International Journal of Heat and Mass Transfer 32 (1989) 1663–1670.